Available online at www.sciencedirect.com

ScienceDirect

journal homepage: www.jfda-online.com

Original Article

A nutraceutical extract from *Inula viscosa* leaves: UHPLC-HR-MS/MS based polyphenol profile, and antioxidant and cytotoxic activities

Nabila Brahmi-Chendouh [a,b,1], *Simona Piccolella* [a,1], *Giuseppina Crescente* [a], *Francesca Pacifico* [a], *Lila Boulekbache* [b], *Sabrina Hamri-Zeghichi* [b], *Salah Akkal* [c], *Khodir Madani* [b], *Severina Pacifico* [a,*]

[a] *Department of Environmental, Biological and Pharmaceutical Sciences and Technologies, University of Campania "Luigi Vanvitelli", Via Vivaldi 43, I-81100, Caserta, Italy*

[b] *Laboratory of 3BS, Faculty of Life and Nature Sciences, University of Bejaia, 06000, Bejaia, Algeria*

[c] *Valorization of Natural Resources, Bioactive Molecules and Biological Analysis Unit, Department of Chemistry, University of Mentouri Constantine 1, 25000, Constantine, Algeria*

ARTICLE INFO

Article history:
Received 23 October 2018
Received in revised form
23 November 2018
Accepted 27 November 2018
Available online 14 January 2019

Keywords:
Chromatography
High pressure liquid
Depsides
Inula
Polyphenols
Tandem mass spectrometry

ABSTRACT

Nowadays, advanced extraction techniques and highly sensitive metabolic profiling methods are effectively employed to get new information on plant chemical constituents. Among them wild medicinal plants or their parts, with large and ancient use in folk medicine, are investigated for their potential functional use and cultivation. In this context, *Inula viscosa* leaves engaged our attention. A simple experimental design, based on Soxhlet extraction and chromatographic fractionation, allowed us to obtain the investigated polyphenol fraction (IvE). UHPLC-HRMS analyses revealed shikimoyl depsides of caffeic acid and unusual dihydrobenzofuran lignans as main secondary metabolites. These compounds, together with cinchonain-type phenols, and hydroxycinnamoyl flavonol glycosides, are reported for the first time in inula. Overall, forty-three secondary metabolites were identified. The extract exerted a remarkable antiradical activity towards DPPH$^{\bullet}$ and ABTS$^{+\bullet}$. Furthermore, it was able to inhibit cell viability and mitochondrial redox activity of neuroblastoma, hepatoblastoma and colon carcinoma cells, whereas it did not affect cell density of HaCaT cells immortalized human keratinocytes. As detected by the oxidant-sensing probe 2′,7′-dichlorodihydrofluorescein diacetate, the inhibitory responses seemed to be related to IvE-induced increase of intracellular reactive oxygen species (ROS). The obtained results highlighted that inula leaves, nowadays even undervalued and unexplored, could be considered a renewable source of nutraceutical compounds.

* *Corresponding author*. Fax: +390823274605.
E-mail address: severina.pacifico@unicampania.it (S. Pacifico).
[1] These authors equally contributed to the work.

https://doi.org/10.1016/j.jfda.2018.11.006

1. Introduction

Inula viscosa (L.) Aiton (syn. *Dittrichia viscosa* (L.) W. Greuter), commonly known as inula, is an annual, herbaceous, perennial plant, belonging to the Asteraceae family, widespread on the slopes of all the Mediterranean coastal regions [1]. The plant is one of the few food sources available to honey bees, which bottled it, thanks to its abundant pollen production and the long flowering. As inula provides unifloral honey in Europe, it represents a low-cost efficient agent of controlling varroosis in *Apis mellifera* colonies [2] and similarly seems to have an active role in the cycle of auxiliary insects that control *Bactrocera oleae*, one of the main pests of olive groves. Indeed, the pest management activity of the plant is just one aspect that makes it unique. In fact, traditional medicine brings in vogue its ability to exert health-promoting effects (e.g. anti-inflammatory, antipyretic and antiseptic) and inula-based preparations are reported as useful and precious remedies. In Morocco *I. viscosa* root and leaf decoction was used to treat hypertension, diabetes mellitus [3], and for the treatment of skin irritations of allergic origin [4]. Several flavonoid constituents were isolated from inula aerial parts and their resinous exudate [5,6]. The antiproliferative, antimicrobial and apoptosis efficacy [7] of some of these compounds and the diversity in hydroxycinnamic acids, namely mono- and dicaffeoylquinic acids, allowed inula leaves to be considered a potential source for food additives and preservatives [8]. Recently, among eleven Algerian medicinal and aromatic plants ^{1}H NMR-based metabolic profiled, *Inula viscosa* appeared mainly constituted of flavonol derivatives [9]. In this context, considering the wide inula use in traditional medicine in Algeria, especially in farming areas for the treatment of various diseases, such as bronchitis, diabetes and injuries and with the aim to provide new insights in *Inula viscosa* leaves as a renewable source of functional ingredients, UHPLC-HR-MS/MS profiling of an inula extract, partially purified, was carried out. The antioxidant and cytotoxic properties were also assessed.

2. Materials and methods

2.1. Reagents

All the solvents used for extraction and fractionation purposes, acetonitrile (LC-MS grade), formic acid (98%, for mass spectrometry) and reagents for Folin–Ciocalteau and DPPH radical scavenging assays were purchased from Sigma–Aldrich (Buchs, Switzerland).

Cell culture media and reagents for cytotoxicity testing were purchased from Invitrogen (Paisley, Scotland, UK). MTT [3-(4,5-dimethyl-2-thiazolyl)-2,5-diphenyl-2H-tetrazolium bromide] and SRB (sulforhodamine B) were from Sigma–Aldrich Chemie GmbH.

2.2. Plant drug extraction and fractionation procedure

Dried leaves of *I. viscosa*, collected in Béjaïa (Algeria) in March 2015, were pulverized by a rotating knives homogenizer and underwent Soxhlet extraction, using firstly chloroform and then methanol as extracting solvents. At the end of each cycle the sample was centrifuged at 5000×*g* for 5 min at 4 °C in an Avant™ J-25 centrifuge (Beckman Coulter, USA), equipped with a JA-14 rotor. The obtained supernatants were dried using a rotary evaporator (Heidolph Hei-VAP Advantage, Germany). Methanol extract was solubilized in pure water and underwent discontinuous liquid–liquid extraction using ethyl acetate, obtaining an aqueous and an organic fraction. This latter was further fractionated by column chromatography (SiO_2 CC; h 6 cm, Ø 1 cm), eluting first with $CHCl_3$, and then with a $CHCl_3$/EtOAc solution (1:1, v/v), pure EtOAc and MeOH. The EtOAc fraction, named *Iv*E (*Inula viscosa* Ethyl acetate), underwent UHPLC-HRMS investigation. The fractionation scheme is depicted in Fig. 1S.

2.3. UHPLC-TOF-MS and TOF-MS^2 analyses

A Shimadzu NEXERA UHPLC system was used with a Luna® Omega Polar C18 column (1.6 μm particle size, 150 × 2.1 mm i.d., Phenomenex, Torrance, CA, USA). Separation was achieved with a linear gradient of water (A) and acetonitrile (B), both with 0.1% formic acid under a linear gradient elution from 2 to 30% B in 17 min. Then, the starting conditions were restored and the column was allowed to re-equilibrate for 2 min. The total run time was 19 min, with a flow rate of 0.5 mL min^{-1} and an injection volume of 2.0 μL.

MS analysis was performed using the AB SCIEX TripleTOF 4600 system with a DuoSpray™ ion source operating in negative electrospray ionization. The APCI probe of the source was used for fully automatic mass calibration using the Calibrant Delivery System (CDS). CDS injects a calibration solution matching polarity of ionization and calibrates the mass axis of the TripleTOF® system in all scan functions used (MS or MS/MS). Data were collected by information dependent acquisition (IDA) using a TOF-MS survey scan of 100–1500 Da (100 ms accumulation time) and eight dependent TOF-MS/MS scans of 80–1250 Da (100 ms accumulation time), using a collision energy (CE) of 45 V with a collision energy spread (CES) of 15 V. All ions which exceeded 50 cps were selected, excluding isotopes within 4 Da and the maximum number of candidate ions to monitor per cycle was set to 8. The following parameter settings were also used: declustering potential (DP), 60 V; ion spray voltage, −4500 V; ion source heater, 600 °C; curtain gas, 35 psi; ion source gas, 45 psi. Data processing was performed using the PeakView® - Analyst® TF 1.7 Software.

2.4. Determination of total phenols

The total phenol amount of EtOAc extract and fractions therefrom, including *Iv*E, was determined according to the Folin–Ciocalteau procedure [10] with slight modifications. Analyzed samples (1.0 mg/mL in DMSO) were mixed with 0.250 mL of the Folin–Ciocalteau reagent (FCR) and 2.25 mL of Na_2CO_3 (7.5% w/v). Tests were carried out performing three replicate measurements for three samples (n = 3) of the extract (in total, 3 × 3 measurements). After stirring the reaction mixture at room temperature for 3 h, 300 μL of each sample were transferred into a multiwell plate and the

absorbance was read at 765 nm using a Wallac Victor^3 multilabel plate reader (PerkinElmer Inc., Waltham, MA). The content of total phenols of the samples was expressed as milligram gallic acid equivalents (GAEs) per g of dried extract.

2.5. Determination of radical scavenging capacity

The assessment of antioxidant and radical scavenging abilities was carried out by applying DPPH and ABTS methods. The activity, estimated for dose levels equal to 3.125, 6.25, 12.5, 25.0, 50.0 and 100.0 μg/mL (final concentration levels), was compared to a blank arranged in parallel to the samples. ABTS [2,2′-azinobis-(3-ethylbenzothiazolin-6-sulfonic acid)] radical cation scavenging capacity and 2,2-diphenyl-1-picrylhydrazyl (DPPH) radical scavenging capability were determined as previously reported [11]. Tests were carried out performing three replicate measurements for three samples (n = 3) of the extract (in total, 3 × 3 measurements). Results are the mean ± SD values. ID_{50} and TEAC (Trolox® Equivalent Antioxidant Capacity) values were also calculated.

2.6. Cytotoxicity assessment

Cytotoxicity assays, which use different parameters associated with cell death and proliferation, were performed. *Iv*E extract stock solution (50.0 mg/mL in EtOH) was further diluted in cell culture medium to appropriate final dose levels. Tests were carried out performing twelve replicate (n = 12) measurements for three samples of each extract (in total: 12 × 3 measurements). Recorded activities were compared to an untreated blank arranged in parallel to the samples. Results are the mean ± SD values.

2.6.1. Cell cultures

Human HaCaT keratinocyte cell line, human SH-SY5Y neuroblastoma cell line, and HCT 116 colorectal carcinoma cell line were purchased from ATCC (American Type Culture Collection). Hepatoblastoma HepG2 cell line was from ICLC (Interlab Cell Line Collection) at Istituto Nazionale per la Ricerca sul Cancro, Genoa (Italy). The cells were grown in DMEM high glucose medium supplemented with 10% Fetal Bovine Serum, 50.0 U/mL penicillin, and 100.0 μg/mL streptomycin, at 37 °C in a humidified atmosphere containing 5% CO_2.

2.6.2. MTT cell viability test

The cells were seeded in 96-multiwell plates at a density of 1.5 × 10^4 cells/well. After 24 h cells were treated with *Iv*E at three dose levels (25.0, 50.0, and 100.0 μg/mL). At 24, 48 and 72 h of incubation, inhibition of mitochondrial redox activity was determined as previously described [12].

2.6.3. SRB cell viability test

The cells were seeded in 96-multiwell plates at a density of 1.5 × 10^4 cells/well. After 24 h of incubation, cells were treated with *Iv*E at three dose levels (25.0, 50.0, and 100.0 μg/mL). At 48 h of incubation, cell viability inhibition (CVI, %) was determined as previously described [13].

2.7. Measurement of intracellular ROS formation

The levels of intracellular Reactive Oxygen Species (ROS) were determined by the change in fluorescence resulting from the oxidation of the fluorescent probe 2′,7′-dichlorofluorescein diacetate (DCFH-DA) [12]. SH-SY5Y cell line was seeded in 96-multiwell plates at a density of 1.5 × 10^4 cells/well. Twenty-four hours after seeding, cells were treated with *Iv*E (2.5, 5.0, 10.0 and 25.0 μg/mL) and incubated for 48 h. Thus, DCFH-DA (10 μM) dissolved in treatment medium was added to each well for 60 min. At the end of incubation, DCFH-DA solution was removed, wells were washed with PBS (100 μL) and the 96-well microplate was placed into a PerkinElmer's Victor^3 Multilabel Plate Reader at 37 °C. The fluorescence intensity was measured at 485 nm excitation and 535 nm emission wavelength after 6 h. Hydrogen peroxide (0.4 mM) was used as positive control for intracellular reactive species production.

2.8. Statistical analysis

Data analyses were performed using GraphPad Instat software (GraphPad PrismInc., San Diego, CA, USA). All data were expressed as mean values ± standard deviation (SD). $P < 0.05$ values or less were considered to indicate statistically significant difference.

3. Results and discussion

The diversity in phenols and polyphenols of *Inula viscosa* leaves was unraveled applying sequential fractionation techniques on extracts from previously defatted and deterpenated materials. The total phenol content (TPC) of fractions obtained, carried out by the Folin–Ciocalteu reagent (FCR) assay, highlighted the constitution of a fraction, namely *Iv*E, whose TPC value, equal to 299.1 ± 34.5 GAE mg per g of dried extract (Fig. 1A), was about 3-fold higher than that previously reported by Mahmoudi and co-workers for an 80% methanol macerated extract from *I. viscosa* leaves [8]. The findings were in line with differences in extraction method, and, in particular, in extracting solvents adopted, so much as *Iv*E TPC value appeared higher (about twice) also in comparison to other data previously described [14] and similar to those related to *I. viscosa* leaf samples collected in Morocco in the region of Sefrou [15]. Indeed, *Iv*E TPC could be a result of a build-up of phenols and polyphenols obtained through fractionation. The *Iv*E radical scavenging capacity was further tested, suggesting a good efficacy in reducing both DPPH radical and ABTS radical cation solutions. Fig. 1B shows the dose-response curves of *Iv*E $DPPH^{\bullet}$ and $ABTS^{\bullet+}$ activities. It was found that the radical-scavenging capabilities increased with the dose level. At 50 μg/mL dose, *Iv*E scavenged $DPPH^{\bullet}$ by 87% while, at same concentration, $ABTS^{\bullet+}$ scavenging effect was equal to 67.4%. The sample antiradical efficacy was highlighted by calculating its dose able to scavenge by 50% (ID_{50} value) both $DPPH^{\bullet}$ and $ABTS^{\bullet+}$ probes. ID_{50} values, which were equal to 14.1 μg mL^{-1} (*vs.* $DPPH^{\bullet}$) and 24.2 μg mL^{-1} (*vs.* $ABTS^{\bullet+}$), together with their relative TEAC values, required further investigation aimed at defining the chemical composition of the antiradical fraction. Thus, in order to identify *Iv*E components, UHPLC-HRMS

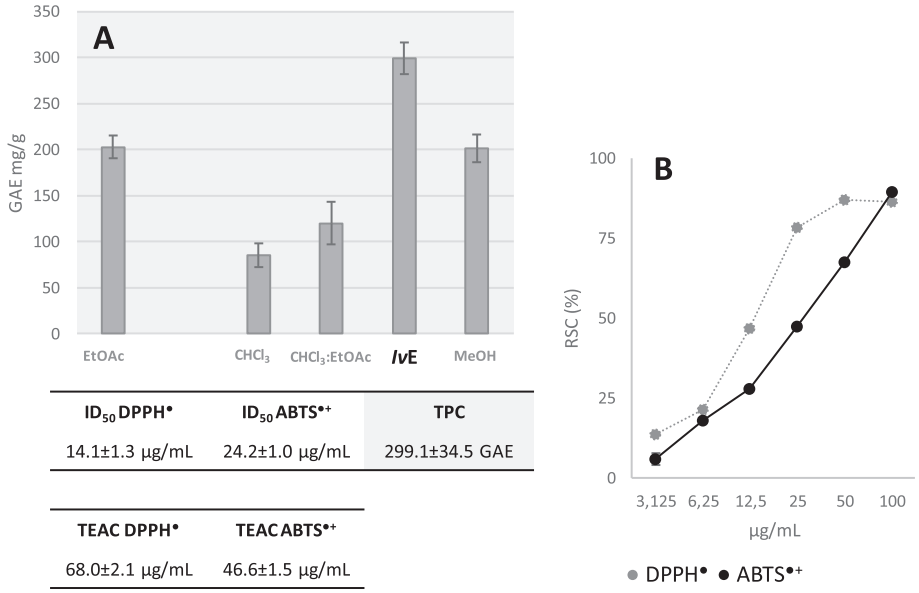

ID_{50} DPPH•	ID_{50} ABTS•+	TPC
14.1±1.3 µg/mL	24.2±1.0 µg/mL	299.1±34.5 GAE

TEAC DPPH•	TEAC ABTS•+
68.0±2.1 µg/mL	46.6±1.5 µg/mL

Fig. 1 – A) Total Phenol Content (TPC) of EtOAc parental extract and fractions therefrom, reported as GAE (Gallic Acid Equivalents mg per g of extract); B) *Iv*E ABTS$^{\bullet+}$ and DPPH$^{\bullet}$ Radical Scavenging Capacity (RSC, %). Values, reported as percentage vs. blank, are the mean ± SD of measurements carried out on 3 samples (n = 3) analyzed three times. ID_{50} values (µg/mL) and TEAC values (Trolox® Equivalents Antioxidant Capacity, µg Trolox® per g of extract) are also reported.

analyses were performed. The analytical method applied, which underwent significant advances in recent years, proving to be highly sensitive and selective in a number of fields, has multiple advantages, currently not fully exploited, over classical unit-mass-resolution tandem mass spectrometry.

3.1. *Iv*E chemical composition

Forty-three compounds were tentatively identified in *Iv*E extract. MS and MS/MS experimental data, recorded in negative ion mode, were summarized in Table 1, together with molecular formulas, and mass accuracy (in ppm). The $[M-H]^-$ ion at *m/z* 341.1086 of compound **1**, together with chloride and formate adduct ions at *m/z* 377.0872 and 387.1165, was in accordance with a disaccharide. Compound **2** was likely shikimic acid. Its $[M-H]^-$ ion at *m/z* 173.0460 ($C_7H_{10}O_5$, 2.6 ppm error *vs.* calculated mass) provided MS/MS diagnostic ions at *m/z* 129.0560 and 111.0450. Metabolite **3**, putatively identified as dihydroxybenzoic acid (e.g. protocatechuic acid), showed the $[M-H]^-$ ion at *m/z* 153.0198, which produced the fragment ion at *m/z* 109.0297 by CO_2 (−44 Da) neutral loss.

Based on the fragmentation pattern (Table 1; Fig. 2S), compound **4** was tentatively identified as 3,7-dihydroxycoumarin. In fact, the deprotonated molecular ion at *m/z* 177.0197 generated product ions at *m/z* 149.0241 ($[M-H-CO]^-$), 133.0294 ($[M-H-CO_2]^-$), 121.0286 ($[M-H-2CO]^-$), 105.0345 ($[M-H-CO-CO_2]^-$) and 93.0345 ($C_6H_5O^-$, calculated mass 93.0346, −1.1 ppm error). Compound **5**, whose $[M-H]^-$ ion was at *m/z* 179.0355, according to the molecular formula $C_9H_8O_4$, was identified as caffeic acid, whereas metabolites **6**–**11** and **32**–**33** could be caffeic acid derivatives. In particular, metabolites **6** and **8** showed the $[M-H]^-$ ion at *m/z* 295.0455 and 295.0458, respectively, according to the elemental composition $C_{13}H_{12}O_8$. The MS/MS ion at *m/z* 115.0038 (or 115.0040) is likely a deprotonated malic acid, formed through the neutral loss of caffeic acid. The presence of this latter was further confirmed by its secondary product ions at *m/z* 179.0349 (or 179.0352), 135.0451 (or 135.0453) and 133.0142 (or 133.0145). Compounds **9**–**11**, exhibiting the same elemental composition ($C_{16}H_{16}O_8$), could be esters between caffeic acid and shikimic acid hydroxyl groups, differing for their esterification site [16]. Based on their LC elution orders, compared with those reported in literature for synthesized caffeoylshikimic acids (CSAs) [17], they were tentatively identified as 5-, 4- and 3-CSA, respectively. Compound **7** was putatively identified as caffeoylquinic lactone (3-CQL) [18]. Compound **33** was a dicaffeoylshikimic acid (diCSA; *m/z* 497.1097 ($C_{25}H_{22}O_{11}$, 1.5 ppm error). The MS^2 product ions at *m/z* 335.0762 ($[M-H-162]^-$), 179.0346 ($[M-H-162-156]^-$), 161.0240 and 135.0451 fortified this hypothesis. The $[M-H]^-$ ion at *m/z* 365.1148 ($C_{20}H_{18}N_2O_5$, 1.4 ppm error) of metabolite **32** allowed us to identify it as *N*-caffeoyl-tryptophan. In fact, the caffeoyl moiety loss yielded the ion at *m/z* 203.0824 (deprotonated tryptophan), which in turn decarboxylated to give the ion at *m/z* 159.0930 [19].

Compounds **12**, **15** and **19**, with $[M-H]^-$ ions at *m/z* 513.1045 (or 513.1046), in accordance to the molecular formula $C_{25}H_{22}O_{12}$ (1.3 and 1.5 ppm error *vs* calculated mass), showed almost superimposable TOF-MS^2 spectra (Fig. 2) and were tentatively identified as isomers of brainic acid, a shikimoyl derivative of blechnic acid widely reported as a characteristic lignan of blechnaceous ferns [20] or *Brainea insignis* [21]. A blechnic acid derivative, which displayed anti-inflammatory activity through inhibiting expression of iNOS and COX-2, was also described as constituent of *Salvia miltiorrhiza* Bunge [22]. In Fig. 3 the proposed fragmentation pathway of compound **12** is reported. Briefly, the TOF-MS^2 spectrum showed

Table 1 – LC-HR-MS/MS data recorded in negative ion mode of metabolites tentatively identified in IvE.

Rt (min)	Tentative assignment	Formula	$[M-H]^-$ found (*m/z*)	$[M-H]^-$ calc. (*m/z*)	Error (ppm)	RDB	MS/MS fragment ions (*m/z*)
0.31	Dihexose **(1)**	$C_{12}H_{22}O_{11}$	341.1086 377.0872 $[M+Cl]^-$ 387.1165 $[M+HCOO]^-$	341.1089	2.5	2	179.0569; 161.0449; 143.0355; 131.0346; 119.0352; 113.0255; 101.0250; 89.0244
0.85	Shikimic acid **(2)**	$C_7H_{10}O_5$	173.0460	173.0455	2.6	3	129.0560; 111.0450; 83.0503; 81.0345
1.78	Dihydroxybenzoic acid **(3)**	$C_7H_6O_4$	153.0198	153.0193	3.1	5	109.0297; 108.0220
4.13	3,7-Dihydroxycoumarin **(4)**	$C_9H_6O_4$	177.0197	177.0193	2.1	7	149.0241; 133.0294; 121.0286; 105.0345; 93.0345; 89.0397
4.25	Caffeic acid **(5)**	$C_9H_8O_4$	179.0355	179.0350	2.9	6	135.0459; 134.0381
5.77	Caffeoyl-malic acid 1 **(6)**	$C_{13}H_{12}O_8$	295.0455	295.0459	−0.5	8	179.0349; 135.0451; 133.0142; 115.0038
5.83	3-CLQ **(7)**	$C_{16}H_{16}O_8$	335.0773	335.0772	0.2	9	179.0350; 161.0248; 135.0452; 133.0300
5.94	Caffeoyl-malic acid 2 **(8)**	$C_{13}H_{12}O_8$	295.0458 591.1002 $[2M-H]^-$	295.0459	−0.5	8	179.0352; 135.0453; 133.0145; 115.0040
5.97	5-CSA **(9)**	$C_{16}H_{16}O_8$	335.0772	335.0772	−0.1	9	179.0355; 135.0458; 134.0378; 133.0298; 111.0455
6.43	4-CSA **(10)**	$C_{16}H_{16}O_8$	335.0772	335.0772	−0.1	9	179.0355; 161.0250; 135.0457; 133.0299
7.30	3-CSA **(11)**	$C_{16}H_{16}O_8$	335.0775	335.0772	0.8	9	179.0361; 161.0253; 135.0460; 133.0301
7.75	Shikimoyl blechnic acid 1 **(12)**	$C_{25}H_{22}O_{12}$	513.1045	513.1039	1.3	15	339.0512; 313.0712; 295.0609; 293.0451; 277.0504; 269.0815; 267.0661; 254.0581; 249.0554; 185.0243; 159.0451; 109.0297
8.24	Cinchonain II **(13)**	$C_{39}H_{32}O_{15}$	739.1668	739.1668	−0.1	24	721.1612; 629.1340; 611.1240; 587.1236; 569.1128; 477.0829; 459.0742; 451.1048; 449.0897; 435.0731; 417.0633; 407.0781; 339.0515; 337.0720; 325.0361; 321.0407; 289.0719; 287.0561; 245.0821; 177.0196; 161.0249; 137.0230
8.59	Cinchonain I **(14)**	$C_{24}H_{20}O_9$	451.1040	451.1035	1.2	15	341.0672; 323.0563; 231.0301; 219.0299; 217.0145; 203.0350; 191.0351; 189.0197; 177.0194; 161.0244; 151.0401; 123.0451; 109.0300
9.06	Shikimoyl blechnic acid 2**(15)**	$C_{25}H_{22}O_{12}$	513.1046	513.1039	1.5	15	339.0525; 312.0733; 295.0625; 293.0468; 277.0523; 269.0833; 267.0663; 254.0589; 249.0562; 239.0724; 185.0255; 159.0460; 109.0303
9.16	Quercetin-O-hexoside 1 **(16)**	$C_{21}H_{20}O_{12}$	463.0886	463.0882	0.9	12	301.0352; 300.0279; 271.0245; 255.0294; 243.0294; 178.9965; 151.0039
9.21	Rutin **(17)**	$C_{27}H_{30}O_{16}$	609.1461	609.1461	0.0	13	301.0346; 300.0267; 271.0236; 255.0286
9.37	Quercetin-O-hexoside 2 **(18)**	$C_{21}H_{20}O_{12}$	463.0889	463.0882	1.5	12	301.0360; 300.0280; 271.0252; 255.0302; 243.0297; 151.0032
9.76	Shikimoyl blechnic acid 3 **(19)**	$C_{25}H_{22}O_{12}$	513.1045	513.1039	1.3	15	339.0515; 313.0720; 295.0612; 293.0453; 277.0509; 269.0819; 267.0663; 254.0584; 249.0557; 239.0712; 185.0249; 159.0457; 147.0454; 109.0300
10.09	Naringenin-7-O-hexoside **(20)**	$C_{21}H_{22}O_{10}$	433.1145	433.1140	1.1	11	313.0726; 271.0620; 177.0215; 165.0394; 151.0042; 119.0505; 107.0142
10.09	Kaempferol-7-O-hexoside 1 **(21)**	$C_{21}H_{20}O_{11}$	447.0937	447.0933	1.2	12	327.0493; 285.0408; 284.0333; 255.0305; 227.0350; 211.0399; 199.0401; 183.0446; 151.0023
10.13	Isorhamnetin-O-pentosylhexoside **(22)**	$C_{27}H_{30}O_{16}$	609.1475	609.1461	2.3	13	315.0515; 314.0433; 300.0278; 299.0202; 271.0248; 255.0291; 243.0307
10.58	Kaempferol-7-O-hexoside 2 **(23)**	$C_{21}H_{20}O_{11}$	447.0941	447.0933	1.8	12	327.0509; 285.0408; 284.0330; 255.0303; 229.0504; 227.0354; 211.0399; 183.0455
10.79	Isorhamnetin-O-rutinoside **(24)**	$C_{28}H_{32}O_{16}$	623.1619	623.1618	0.2	13	315.0516; 314.0433; 300.0287; 299.0204; 271.0253
10.81	Quercetin-3-O-(6″-acetyl) hexoside **(25)**	$C_{23}H_{22}O_{13}$	505.0993	505.0988	1.1	13	463.0907; 301.0362; 300.0286; 271.0254; 255.0302; 243.0298; 227.0348; 178.9991; 151.0043
11.23	Kaempferol-3-O-pentoside **(26)**	$C_{20}H_{18}O_{10}$	417.0827	417.0827	0	12	285.0398; 284.0323; 255.0296; 227.0343
11.56	Decarboxylated shikimoyl blechnic acid **(27)**	$C_{24}H_{22}O_{10}$	469.1148	469.1140	1.7	14	295.0615; 293.0458; 277.0511; 269.0820; 267.0665; 254.0587; 249.0561; 239.0715; 185.0248; 159.0456; 147.0454; 137.0248; 109.0299; 93.0350
12.11	Quercetin-O-(caffeoyl)-hexoside **(28)**	$C_{30}H_{26}O_{15}$	625.1189	625.1199	−1.6	18	463.0908; 323.0784; 301.0360; 300.0280; 271.0251; 255.0301; 243.0305; 178.9989; 161.0246; 151.0037
12.13	Kaempferol-O-deoxyhexoside **(29)**	$C_{21}H_{20}O_{10}$	431.0993	431.0984	2.2	12	285.0412; 284.0336; 255.0306; 245.0452; 239.0364; 229.0512; 227.0356; 211.0399; 183.0449; 135.0452

12.21	Dihydrokaempferol **(30)**	$C_{15}H_{12}O_6$	287.0562	287.0561	0.3	10	151.0032; 135.0453; 134.0373; 107.0137
12.58	Kaempferol-*O*-acetylhexoside **(31)**	$C_{23}H_{22}O_{12}$	489.1048	489.1039	1.9	13	285.0413; 284.0332; 255.0305; 227.0355
12.99	N-caffeoyl-tryptophan **(32)**	$C_{20}H_{18}N_2O_5$	365.1148 731.2381 $[2M-H]^-$	365.1143	1.4	13	229.0618; 203.0824; 186.0558; 161.0242; 159.0930; 142.0662; 135.0453; 133.0297
13.42	diCSA **(33)**	$C_{25}H_{22}O_{11}$	497.1097	497.1089	1.5	15	335.0762; 255.0654; 211.0759; 179.0346; 161.0240; 135.0451
13.46	Kaempferol-3-*O*-(caffeoyl)-hexoside **(34)**	$C_{30}H_{26}O_{14}$	609.1271	609.1250	3.5	18	447.0958; 323.0779; 285.0405; 284.0351; 255.0304; 221.0456; 179.0353; 161.0247; 135.0452
13.60	Quercetin-*O*-*p*-coumaroyl-*O*-hexoside 1 **(35)**	$C_{30}H_{26}O_{14}$	609.1270	609.1250	3.3	18	463.0906; 301.0361; 300.0281; 271.0252; 255.0302; 178.9983; 151.0033
13.77	Quercetin-*O*-feruloyl-*O*-hexoside **(36)**	$C_{31}H_{28}O_{15}$	639.1362	639.1355	1.0	18	477.1055; 463.0900; 315.0508; 301.0356; 300.0275; 271.0250; 255.0300; 243.0295; 178.9986; 151.0037
13.81	Quercetin-*O*-*p*-coumaroyl-*O*-hexoside 2 **(37)**	$C_{30}H_{26}O_{14}$	609.1267	609.1250	2.8	18	463.0908; 301.0364; 300.0283; 271.0257; 255.0304; 178.9987; 151.0038
14.67	Kaempferol-*O*-*p*-coumaroyl-*O*-hexoside **(38)**	$C_{30}H_{26}O_{13}$	593.1305	593.1301	0.7	18	447.0945; 285.0400; 284.0321; 255.0296; 227.0345; 145.0288
14.89	Kaempferol-*O*-(feruloyl)-hexoside 1 **(39)**	$C_{31}H_{28}O_{14}$	623.1404	623.1406	−0.4	18	447.0952; 337.0933; 323.0778; 299.0567; 285.0409; 284.0332; 255.0302; 227.0349; 193.0508; 179.0350; 161.0242
14.93	Kaempferol-*O*-(*p*-coumaroyl)-hexoside 1 **(40)**	$C_{30}H_{26}O_{13}$	593.1304	593.1301	0.6	18	447.0968; 307.0835; 285.0409; 284.0333; 255.0305; 227.0354; 145.0304
15.16	Kaempferol-*O*-(feruloyl)-hexoside 2 **(41)**	$C_{31}H_{28}O_{14}$	623.1404	623.1406	−0.4	18	447.0956; 337.0937; 323.0777; 299.0566; 285.0403; 284.0326; 255.0301; 227.0352; 193.0508; 179.0352; 161.0245
15.31	Kaempferol-*O*-(*p*-coumaroyl)-hexoside 2 **(42)**	$C_{30}H_{26}O_{13}$	593.1300	593.1301	−0.1	18	447.0959; 307.0828; 285.0407; 284.0331; 255.0305; 227.0354; 145.0300
15.70	Kaempferol-*O*-(feruloyl)-hexoside 3 **(43)**	$C_{31}H_{28}O_{14}$	623.1410	623.1406	0.6	18	447.0965; 337.0934; 323.0779; 299.0565; 285.0409; 284.0332; 255.0303; 227.0350

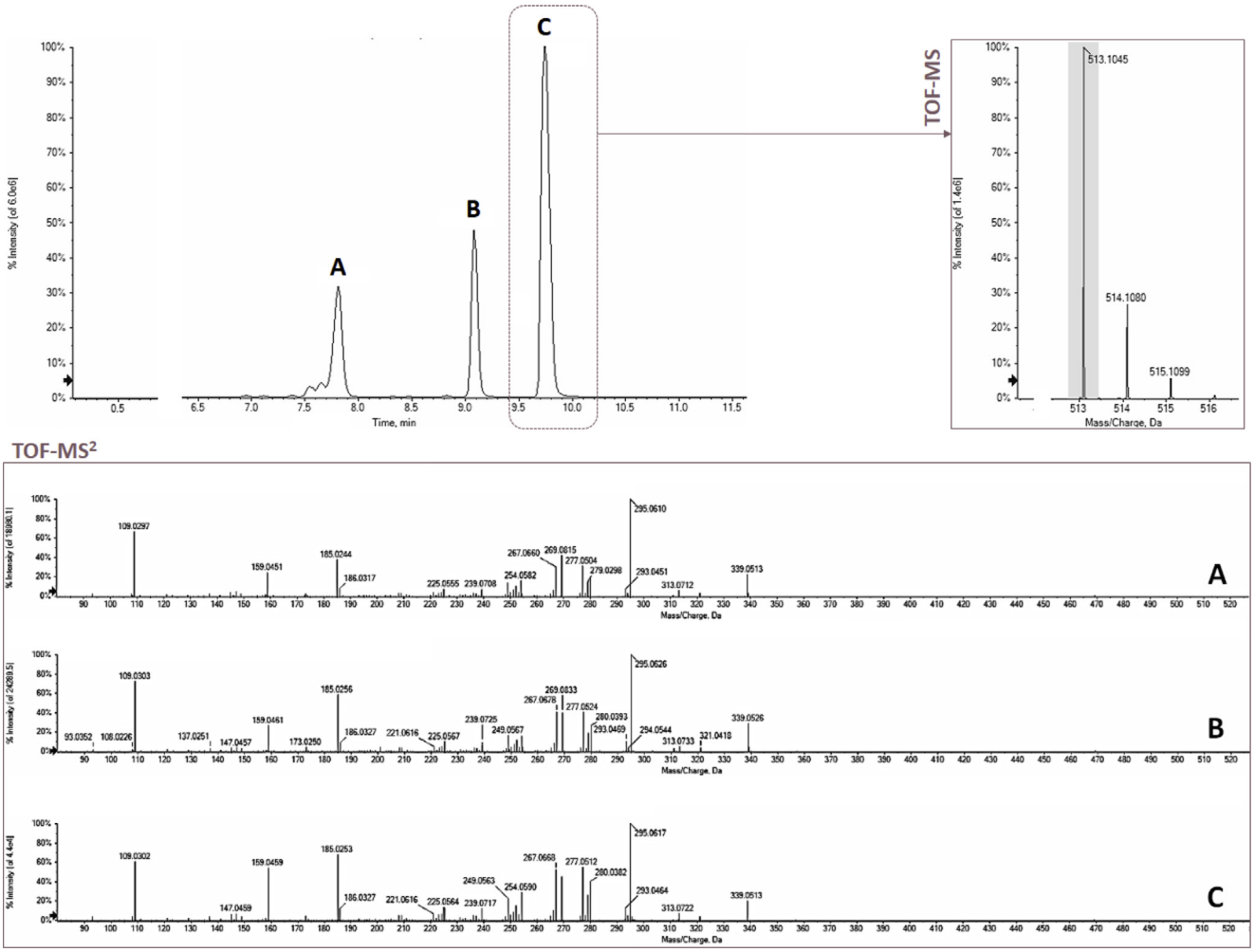

Fig. 2 – XIC, TOF-MS and TOF-MS^2 spectra of compounds A) 12, B) 15 and C) 19.

the ion at *m/z* 339.0512 ($C_{18}H_{11}O_7^-$, 0.59 ppm error) deriving from the neutral loss of shikimic acid (174.0528 Da). This latter decarboxylated to give the base peak at *m/z* 295.0609, which in turn gave rise to the ion at *m/z* 185.0243 after the loss of the catechol moiety ($C_6H_6O_2$). Alternatively, the ion at *m/z* 269.0815 was generated after an electron rearrangement leading to the neutral loss of 200.0327 Da ($C_8H_8O_6$) and of a CO_2 molecule, and subsequently fragmented to yield product ions at *m/z* 159.0451 ($C_{10}H_7O_2^-$), 147.0455 ($C_9H_7O_2^-$) and 109.0297 ($C_6H_5O_2^-$). Recently, another lignan compound, medioresinol, was tentatively identified in inula leaves [23], suggesting that the plant is an unexplored but rich source of lignans. To strengthen this hypothesis, metabolite **27** was in accordance with a decarboxylated brainic acid derivative. The deprotonated molecular ion at *m/z* 469.1148 dissociated providing the ion at *m/z* 295.0615 as base peak, due to the neutral loss of shikimic acid.

Metabolites **13** and **14** were tentatively identified as flavan-3-ols with a cinchonain-type phenylpropanoid substitution. HRMS data recorded for compound **13** were in accordance with the presence of deprotonated cinchonain II (*m/z* 739.1668, $C_{39}H_{32}O_{15}$, -0.1 ppm error). The fragmentation of the $[M\text{-}H]^-$ ion gave rise to diagnostic product ions, arising from retro-Diels-Alder reactions, phenyl cleavage and interflavan fission. The deprotonated molecular ion for compound **14** at *m/z* 451.1040 was in accordance with a molecular formula $C_{24}H_{20}O_9$ (1.2 ppm error). The TOF-MS^2 spectrum showed main fragment ions at *m/z* 341.0672, 217.0145, 189.0197 and 177.0194, which could be attributable to cinchonain I [24]. The full fragmentation pathways proposed for these metabolites were reported in Figs. 3S–4S.

Metabolites **16**, **17** and **18** were identified as quercetin glycosides. The comparison with pure reference compounds allowed to characterize compound **17** ($C_{27}H_{30}O_{16}$, 0 ppm error) as rutin, and compound **16** as isoquercetrin. Metabolite **18** was another hexosyl derivative of quercetin. A further derivative of quercetin is metabolite **25**, characterized by a deprotonated molecular ion at *m/z* 505.0993 and, in the TOF-MS^2 experiment, by fragment ions at *m/z* 301.0362 and 300.0286 (as base peak). The relative abundance of the $[\text{aglycone-H}]^{-\bullet}$ ion and the neutral loss of a 204.0631 Da residue ($[M\text{-H-42-162}]^-$) allowed us to tentatively identify this compound as quercetin-3-O-(6″-acetyl) hexoside. Metabolites **22** and **24** were tentatively identified as isorhamnetin glycosides. The fragmentation pattern of the $[M\text{-H}]^-$ ion of **22** highlighted the neutral loss of a disaccharide moiety formed by a pentose and a hexose

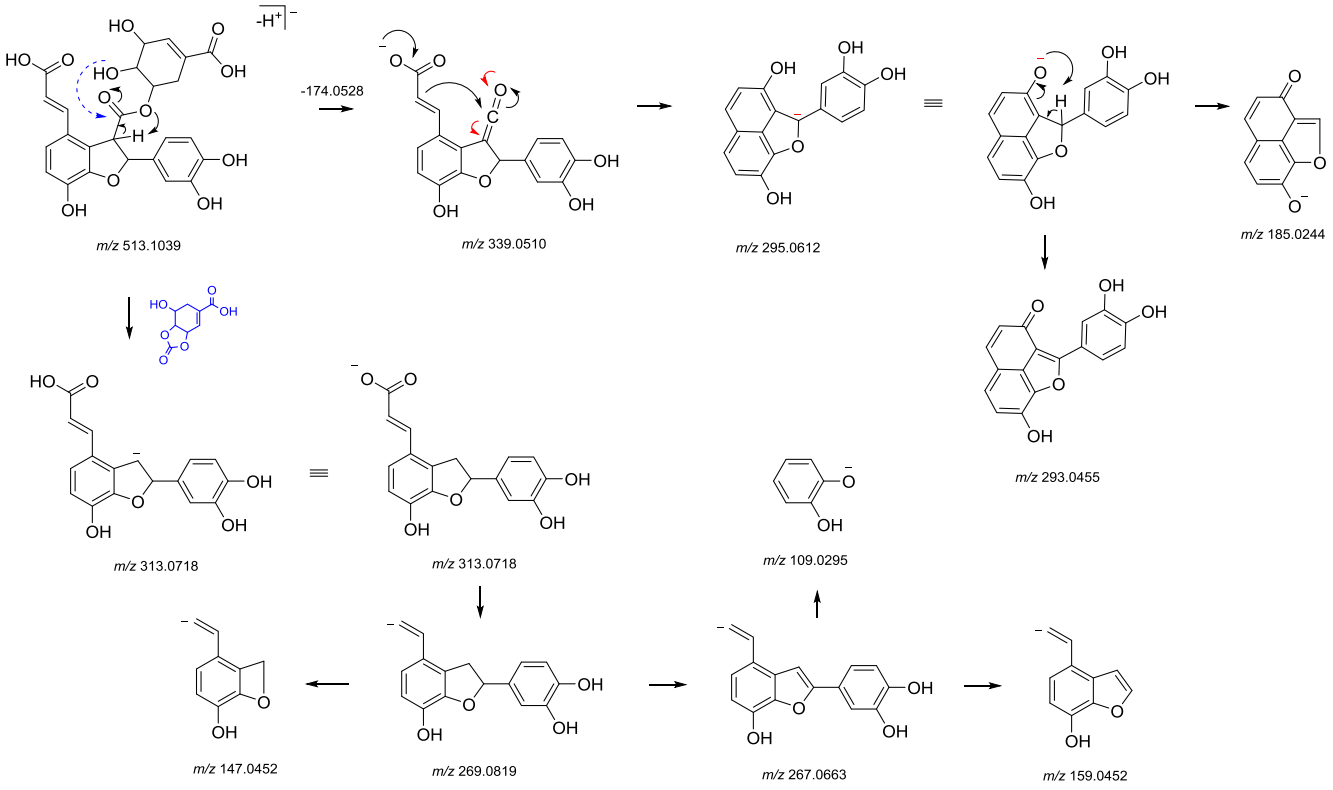

Fig. 3 – Putative fragmentation pathway of compound 12. Measured exact mass of each fragment ion, as listed in Table 1, was at *m/z* within 5 ppm *vs.* its relative theoretical *m/z* value. This latter is reported below each structure.

unit (294.0960 Da, $C_{11}H_{18}O_9$) to give the aglycone ion at *m/z* 315.0515, whereas rutinose was detected as neutral loss of 308.1103 (−1.29 ppm error *vs.* calculated mass) in **24**.

Metabolite **20** could be a naringenin-7-*O*-hexoside ($C_{21}H_{22}O_{10}$, 1.1 ppm error). The TOF-MS^2 fragmentation provided ^{0,2}X ions at *m/z* 313.0726 ([M-H-120]$^-$), besides the deprotonated naringenin at *m/z* 271.0620 ([M-H-162]$^-$) according to 7-*O*-glycosylation [25].

Kaempferol glycosides **21** and **23** differed for the nature of their saccharidic moiety and/or for the glycosylation position. In particular, also in this case, in addition to product ions at *m/z* 285.0408 (Y_0^-) and 284.0333 (or 284.0330) ([Y_0-H]$^{\cdot-}$), less intense X$^-$-type fragment ions were observed at *m/z* 327.0493 (or 327.0509) as a result of bond cleavages in the hexose moiety (^{0,2}X fragmentation). The TOF-MS spectrum of metabolite **26** showed a deprotonated molecular ion at *m/z* 417.0827 ($C_{20}H_{17}O_{10}^-$) and TOF-MS^2 fragment ions comparable to those detected for the previously described compounds, with respect to relative intensity and *m/z* value. The neutral loss of 132.0429 Da likely indicated the presence of a pentose bound to kaempferol by an *O*-glycosidic bond. The same flavonol was generated for compound **29**, following the neutral loss of 146.0581 (1.4 ppm error vs calculated mass) Da, according to the presence of kaempferol-*O*-deoxyhexoside ($C_{21}H_{20}O_{10}$). Compound **30** has been putatively identified as dihydrokaempferol, also named aromadendrin, whereas metabolite **31** could be a kaempferol-3-*O*-(6″-acetyl) hexoside. Aromadendrin (**30**) has been previously reported as a constituent of *Inula graveolens* [26], and aromadendrin derivatives have been detected among other flavonoids in *Inula viscosa* aerial parts exudate [6]. The HRMS analysis of **30** provided the [M-H]$^-$ ion at *m/z* 287.0562 ($C_{15}H_{12}O_6$, 0.3 ppm error *vs.* calculated mass) and product ions at *m/z* 151.0032 and 135.0453, resulting from a cross ring cleavage of C-ring between O1-C2 and C2-C3 bonds.

Metabolites **34**–**43** were tentatively identified as hydroxycinnamoyl derivatives of *O*-glycosyl quercetin or kaempferol. To the best of our knowledge, these metabolites are not very common in *Inula* species. In fact, despite quercetin-3-*O*-β-(6″-caffeoylgalactopyranoside) has been recently isolated and characterized in *Inula ensifolia* aerial parts [27], they have not been detected in *Inula viscosa* until now. Three groups of isobar compounds were detected. The first one included compounds **34**, **35** and **37** characterized by the molecular formula $C_{30}H_{26}O_{14}$. The TOF-MS^2 spectra allowed us to discriminate among them. In fact, compound **34** gave the product ion at *m/z* 447.0958 ([M-H-$C_9H_6O_3$]$^-$), corresponding to kaempferol-*O*-hexoside, which in turn fragmented to yield the deprotonated kaempferol at *m/z* 285.0405/284.0351. Their intensity ratio suggested the C-3 glycosylation. Furthermore, the fragment at *m/z* 323.0779 ($C_{15}H_{15}O_8^-$, 2.2 ppm error vs calculated mass) was pivotal to identify the caffeoylhexose moiety. Thus, it was characterized as kaempferol-3-*O*-(caffeoyl)-hexoside. Similarly, compound **28** was putatively identified as quercetin-*O*-(caffeoyl)-hexoside. The $C_{15}H_{15}O_8^-$ product ion was detected, besides the fragments at *m/z* 463.0908 ([M-H-caffeoyl]$^-$), 301.0360 (deprotonated quercetin) and 300.0280 (deprotonated radical quercetin). The other detected ions were those typical of quercetin, as regards *m/z* ratio and relative intensity.

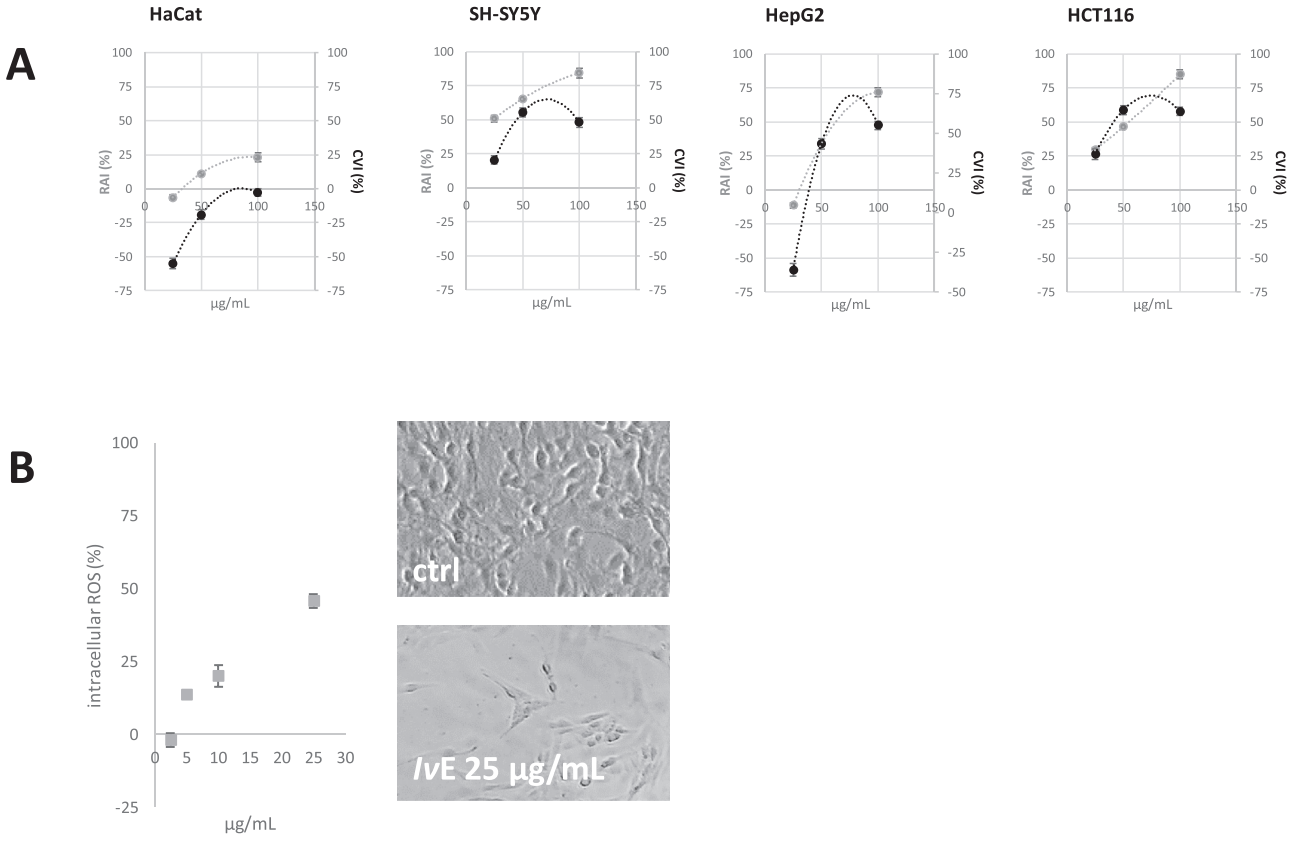

Fig. 4 – A) Mitochondrial redox activity inhibition (RAI %) by MTT and cell viability inhibition (CVI %) by SRB tests in HaCaT, SH-SY5Y, HepG2 and HCT 116 cell lines. Values, reported as percentage vs. an untreated control, represent mean ± standard deviation (SD) of measurements carried out in 3 samples (n = 3) analyzed twelve times. B) Increase of intracellular ROS levels in SH-SY5Y cells exposed to 2.5, 5, 10 and 25 µg/mL *Iv*E dose levels for 48 h. Values are expressed as mean percentage ± SD from measurements carried out on 3 samples (n = 3) analyzed 6 times. *Iv*E-treated cells were observed by Inverted phase contrast and brightfield Zeiss Primo Vert Microscope and representative images were acquired without specific staining.

On the contrary, the fragmentation pattern of metabolites **35** and **37** was in accordance with the presence of two isomers of quercetin-*O*-*p*-coumaroyl-*O*-hexoside. In fact, in both cases the $[M\text{-}H]^-$ ion gave rise to the ions at *m/z* 463.0906 (or 463.0908), 301.0361 (or 301.0364) and 300.0281 (or 300.0283), after the subsequent neutral losses of the *p*-coumaroyl ($C_9H_6O_2$) and hexosyl ($C_6H_{10}O_5$) moiety, respectively. The absence of the product ion at *m/z* 307.0823 ($C_{15}H_{15}O_7^-$) suggested that the *p*-coumaric acid and the hexose were bound to quercetin at different positions, and not linked one to another. A similar fragmentation pattern was observed for metabolite **36**, whose deprotonated molecular ion at *m/z* 639.1362 (1.0 ppm error *vs* calculated mass), was in accordance with the molecular formula $C_{31}H_{28}O_{15}$. The neutral loss of 176.0472 ($C_{10}H_8O_3$, -0.57 ppm error) to yield the ion at *m/z* 463.0900 could correspond to a ferulic acid moiety, allowing us to tentatively identify metabolite **36** as a feruloyl derivative of quercetin-*O*-hexoside.

The second group of isobar compounds included metabolites **38**, **40** and **42** characterized by the molecular formula $C_{30}H_{26}O_{13}$. Despite the presence in all the TOF-MS^2 spectra of fragment ions deriving from the neutral loss of a *p*-coumaroyl ($C_9H_6O_2$) and a hexosyl ($C_6H_{10}O_5$) moiety, only for the first compound the ion at *m/z* 307.0835 ($C_{15}H_{15}O_7^-$, 3.9 ppm error *vs* calculated mass) was not detected, suggesting two different bond positions, as previously discussed for quercetin derivatives. Instead, mass spectra of compounds **40** and **42** appeared almost superimposable.

Metabolites **39**, **41** and **43** were tentatively identified as kaempferol-*O*-(feruloyl)-hexoside isomers, which could differ for the hexose and/or the position of the *O*-glycosidic bond. In accordance with the previous discussion regarding acylated flavonols, the presence of the TOF-MS^2 ion at *m/z* 337.0937 (or 337.0934, $C_{16}H_{17}O_8^-$) could be due to a feruloylhexose moiety. In addition, the less abundant ions at *m/z* 299.0566 and 323.0778 could suggest that the hexose moiety bound the aglycone through the hydroxyl group at position C-6′. The hypothesized fragmentation pathway for compound **43** is depicted in Fig. 5S.

3.2. *IvE cytotoxicity*

The abundance in phenol and polyphenol compounds, as well as the *Iv*E antiradical efficiency, paved the way for testing its potential cytotoxicity. MTT test was carried out on one human normal cell line (HaCaT cells) and three human tumor cell lines

(Fig. 4A). The mitochondrial redox activity of neuroblastoma, epatoblastoma and colorectal carcinoma cell lines was markedly affected by *Iv*E, and, with the sole exception of HepG2 cells, already at the lowest tested dose level (25 μg/mL). The cytotoxic potential, which appeared strongly dose-dependent, was confirmed by the more sensitive and accurate SRB test (Fig. 4A). In fact, after 48 h exposure time, the extract was able to notably reduce cell density and the effect was more pronounced when the 50 μg/mL dose was tested. Indeed, SRB curve was in line to an hormetic dose-response curve showing low-dose stimulatory and high-dose inhibitory responses (inverted U-shaped curve) [28]. The double-edged sword behaviour of polyphenols, and the ability of polyphenols to act as pro-oxidant, could be involved in the observed effect. To underline this hypothesis, because of high metabolic rate and inefficient defense mechanisms neuronal cells are considered to be particularly vulnerable to oxidative stress, *Iv*E-induced increase in intracellular ROS formation was determined in SH-SY5Y cells by fluorescent probe 2′,7′-dichlorofluorescein diacetate. ROS genesis was increased, after 48 h exposure time, by 45.8% (Fig. 4B) suggesting that *Iv*E could modulate endogenous cellular defense mechanisms via stress response. The cytotoxic activity of some common inula constituents, such as nepetin, 3-*O*-methylquercetin, 3,3′-di-*O*-methylquercetin, and hispidulin was broadly investigated [7], whereas other beneficial effects were attributed to its antioxidant dihydroflavonols, which were found to inhibit the production of LTB4, acting directly on the 5-LOX enzyme, and regulating secretory processes such as elastase release [29]. However, the large part of these compounds were not present in the prepared extract, which, as revealed by UHPLC-HRMS analysis, was further rich in caffeoyl shikimic acids. Never reported before in inula, they have been recently shown as inhibitors regulating the early steps of monolignol [30] and unusual dihydrobenzofuran lignans. The potential involvement of these metabolites, as well as of the different cinnamoyl flavonols, in the activity exercise should not be disregarded.

4. Conclusions

LC-HRMS analysis deeply unraveled the chemical composition of an *Inula viscosa* leaf extract, highlighting its diversity in polyphenol constituents, never described before. Antioxidant and cell viability assessment encourage the employment of this wild renewable source for the obtainment of bioactive nutraceutical phytochemicals.

Appendix A. Supplementary data

Supplementary data to this article can be found online at https://doi.org/10.1016/j.jfda.2018.11.006.

REFERENCES

[1] Seca AM, Grigore A, Pinto DC, Silva AM. The genus Inula and their metabolites: from ethnopharmacological to medicinal uses. J Ethnopharmacol 2014;154:286–310.

[2] Sofou K, Isaakidis D, Spyros A, Büttner A, Giannis A, Katerinopoulos HE. Use of costic acid, a natural extract from *Dittrichia viscosa*, for the control of Varroa destructor, a parasite of the European honey bee. Beilstein J Org Chem 2017;13:952–9.

[3] Tahraoui A, El-Hilaly J, Israili ZH, Lyoussi B. Ethnopharmacological survey of plants used in the traditional treatment of hypertension and diabetes in south-eastern Morocco (Errachidia province). J Ethnopharmacol 2007;110:105–17.

[4] Passalacqua NG, Guarrera PM, De Fine G. Contribution to the knowledge of the folk plant medicine in Calabria region (Southern Italy). Fitoterapia 2007;78:52–68.

[5] Grande M, Piera F, Cuenca A, Torres P, Bellido IS. Flavonoids from *Inula viscosa*. Planta Med 1985;51:414–9.

[6] Wollenweber E, Mayer K, Roitman JN. Exudate flavonoids of *Inula viscosa*. Phytochemistry 1991;30:2445–6.

[7] Talib WH, Zarga MHA, Mahasneh AM. Antiproliferative, antimicrobial and apoptosis inducing effects of compounds isolated from *Inula viscosa*. Molecules 2012;17:3291–303.

[8] Mahmoudi H, Hosni K, Zaouali W, Amri I, Zargouni H, Hamida NB, et al. Comprehensive phytochemical analysis, antioxidant and antifungal activities of *Inula viscosa* Aiton leaves. J Food Saf 2016;36:77–88.

[9] Brahmi N, Scognamiglio M, Pacifico S, Mekhouke A, Madani K, Fiorentino A, et al. ^{1}H NMR based metabolic profiling of eleven Algerian aromatic plants and evaluation of their antioxidant and cytotoxic properties. Food Res Int 2015;76:334–41.

[10] Pacifico S, Galasso S, Piccolella S, Kretschmer N, Pan S-P, Nocera P, et al. Winter wild fennel leaves as a source of a source of anti-inflammatory and antioxidant polyphenols. Arab J Chem 2018;11:513–24.

[11] Pacifico S, Piccolella S, Galasso S, Fiorentino A, Kretschmer N, Pan S-P, et al. Influence of harvest season on chemical composition and bioactivity of wild rue plant hydroalcoholic extracts. Food Chem Toxicol 2016;90:102–11.

[12] Piccolella S, Nocera P, Carillo P, Woodrow P, Greco V, Manti L, et al. An apolar *Pistacia lentiscus* L. leaf extract: GC-MS metabolic profiling and evaluation of cytotoxicity and apoptosis inducing effects on SH-SY5Y and SK-N-BE (2) C cell lines. Food Chem Toxicol 2016;95:64–74.

[13] Pacifico S, Piccolella S, Papale F, Nocera P, Lettieri A, Catauro M. A polyphenol complex from *Thymus vulgaris* L. plants cultivated in the Campania Region (Italy): new perspectives against neuroblastoma. J Funct Foods 2016;20:253–66.

[14] Rhimi W, Ben Salem I, Immediato D, Saidi M, Boulila A, Cafarchia C. Chemical composition, antibacterial and antifungal activities of crude *Dittrichia viscosa* (L.) Greuter leaf extracts. Molecules 2017;22:942.

[15] Chahmi N, Anissi J, Jennan S, Farah A, Sendide K, El Hassouni M. Antioxidant activities and total phenol content of *Inula viscosa* extracts selected from three regions of Morocco. Asian Pac J Trop Biomed 2015;5:228–33.

[16] Zhang SH, Hu X, Shi SY, Huang LQ, Chen W, Chen L, et al. Typical ultraviolet spectra in combination with diagnostic mass fragmentation analysis for the rapid and comprehensive profiling of chlorogenic acids in the buds of *Lonicera macranthoides*. Anal Bioanal Chem 2016;408:3659–72.

[17] Jaiswal R, Sovdat T, Vivan F, Kuhnert N. Profiling and characterization by LC-MS^{n} of the chlorogenic acids and hydroxycinnamoylshikimate esters in maté (*Ilex paraguariensis*). J Agric Food Chem 2010;58:5471–84.

[18] Jaiswal R, Matei MF, Subedi P, Kuhnert N. Does roasted coffee contain chlorogenic acid lactones or/and cinnamoylshikimate esters? Food Res Int 2014;61:214–27.

[19] Llorent-Martínez EJ, Spínola V, Gouveia S, Castilho PC. HPLC-ESI-MS^n characterization of phenolic compounds, terpenoid saponins, and other minor compounds in *Bituminaria bituminosa*. Ind Crop Prod 2015;69:80–90.
[20] Wada H, Kido T, Tanaka N, Murakami T, Saiki Y, Chen CM. Chemical and chemotaxonomical studies of ferns. LXXXI. Characteristic lignans of *Blechnaceous* ferns. Chem Pharm Bull 1992;40:2099–101.
[21] Wang K, Li MM, Chen XQ, Peng LY, Cheng X, Li Y, et al. Phenolic constituents from *Brainea insignis*. Chem Pharm Bull 2010;58:868–71.
[22] Gao H, Sun W, Zhao J, Wu X, Lu J-J, Chen X, et al. Tanshinones and diethyl blechnics with anti-inflammatory and anti-cancer activities from *Salvia miltiorrhiza* Bunge (Danshen). Sci Rep 2016;6:33720.
[23] Kheyar-Kraouche N, da Silva AB, Serra AT, Bedjou F, Bronze MR. Characterization by liquid chromatography-mass spectrometry and antioxidant activity of an ethanolic extract of *Inula viscosa* leaves. J Pharmaceut Biomed Anal 2018;156:297–306.
[24] Zhang L, Tu ZC, Xie X, Lu Y, Wang ZX, Wang H, et al. Antihyperglycemic, antioxidant activities of two *Acer palmatum* cultivars, and identification of phenolics profile by UPLC-QTOF-MS/MS: new natural sources of functional constituents. Ind Crop Prod 2016;89:522–32.
[25] March RE, Lewars EG, Stadey CJ, Miao XS, Zhao X, Metcalfe CD. A comparison of flavonoid glycosides by electrospray tandem mass spectrometry. Int J Mass Spectrom 2006;248:61–85.
[26] Sevil O. A eudesmanolide and other constituents from *Inula graveolens*. Phytochemistry 1992;31:195–7.
[27] Stojakowska A, Malarz J, Zubek S, Turnau K, Kisiel W. Terpenoids and phenolics from *Inula ensifolia*. Biochem Syst Ecol 2010;38:232–5.
[28] Calabrese V, Cornelius C, Trovato A, Cavallaro M, Mancuso C, Di Rienzo L, et al. The hormetic role of dietary antioxidants in free radical-related diseases. Curr Pharmaceut Des 2010;16:877–83.
[29] Hernández V, Recio MC, Máñez S, Giner RM, Ríos JL. Effects of naturally occurring dihydroflavonols from *Inula viscosa* on inflammation and enzymes involved in the arachidonic acid metabolism. Life Sci 2007;81:480–8.
[30] Lin CY, Wang JP, Li Q, Chen HC, Liu J, Loziuk P, et al. 4-Coumaroyl and caffeoyl shikimic acids inhibit 4-coumaric acid: coenzyme A ligases and modulate metabolic flux for 3-hydroxylation in monolignol biosynthesis of *Populus trichocarpa*. Mol Plant 2015;8:176–87.